JOURNAL OF MATERIALS SCIENCE **37** (2002) 4775–4782

Analysis of a shear-lag model with nonlinear elastic stress transfer for sequential cracking of polymer coatings

U. A. HANDGE
Institute of Polymers, Department of Materials, ETH Zürich, ML J 16, 8092 Zürich, Switzerland

Analyzing a shear-lag model, the evolution of the fragment size distribution in the sequential cracking of polymer coatings under uniaxial loading is investigated. This study elucidates the role of a nonlinear elastic stress transfer mechanism at the interface on the fragmentation kinetics. Using a nonlinear expression for the shear stress at the interface, analytical expressions for the stress and the strain in the coating are derived. In the initial stage of cracking, the strain in a fragment equals the substrate's strain everywhere except in the exclusion zone at the fragments' edges. In the later stages of fragmentation, the stress and the strain in a fragment attain a universal scaling form with pronounced maxima in the centers of the fragments. Assuming a three parameter Weibull distribution for the statistical distribution of the coating's strength, analytical expressions for the fragment size distribution in the initial stage and numerical results for the fragment size distribution in the later stages of the cracking process are derived.

1. Introduction

The sequential cracking of coatings and surface layers is a phenomenon that appears in a wide range of length scales. Examples are the fragmentation of thin brittle coatings and paint layers [1–10], the cracking of mud during drying [11] and the fragmentation phenomena in geological systems [12]. In general, the multiple breaking of a coating results in a pattern of cracks with an irregular crack spacing. These patterns often consist of polygons and can be characterized by the distribution of the fragment size being a function of time (e.g., in desiccation processes) or applied strain (e.g., in mechanical tests). This distribution of crack spacings reveals that the coating is a disordered system. The disorder can arise from the distribution of defects in the material which are created during preparation of the composite and which promote cracking, spatially varying coating thickness [13], the presence of fillers in the coating etc.. Because of the inhomogeneous structure of the coating, the local strength of the coating is a random quantity, and failure is associated both with the value of the local stress and strain in the coating and the value of the local strength. In general, the distribution of the local strength of the coating is *a priori* unknown [14, 15], and assumptions must be made for the failure probability. In this context, the weakest link approach has become a popular model for the description of failure of materials [16–18].

The values of the local stress and strain in the coating are determined by the specific behaviour of the materials of the coating and the substrate and of the interface under deformation, i.e., the character of deformation (e.g., elastic, plastic or hysteretic) and their stress–strain relation. Materials under deformation depict different kinds of behaviour ranging from linear elastic to highly nonlinear plastic behaviour as well as viscoelastic or hysteretic response. For example, polymers and thus polymer coatings often show a nonlinear response to deformation. Moreover the stress transfer at the interface plays a key role for the sequential breaking of coatings. Since the fragmentation kinetics are strongly influenced by the parameters which describe the material properties, the interfacial properties and the scattering of the local strength, the fragmentation test performed with coatings and fibres embedded in a matrix has become a tool for characterizing the properties of the coating-substrate and fibre-matrix system respectively [19]. In this paper, the fragmentation of polymer coatings that adhere to a substrate is investigated by considering a one-dimensional shear-lag model. We focus on the kinetics of fragmentation, i.e., the evolution of the fragment size distribution with the applied strain. In this study we assume that coating, substrate and interface display elastic response to deformation and thus have a reversible stress–strain relation. It is the aim of this paper to elucidate the role of nonlinear elastic stress transfer at the interface on the fragment size distribution. We clarify the interplay between nonlinearity and disorder by showing that the scaling exponents in the fragmentation kinetics are simple functions of the disorder and nonlinearity parameters of the coating-substrate system. Starting from a shear-lag model, analytical and numerical results are presented which can be compared with experimental data. One can infer from

such a comparison information about the distribution of the coating's strength and the mechanical properties of the interface. Therefore the fragmentation test is an adequate tool in order to characterize polymer coatings.

The paper is organized as follows: First the model for the fragmentation of polymer coatings is presented and the stress and the strain within a fragment is calculated. Then the sequential cracking of the coating using a three parameter Weibull distribution for the coating's strength in the initial and in the later stages of fragmentation is investigated. We focus on the evolution of the fragment size distribution with the applied strain and discuss the influence of the disorder and material parameters on the fragmentation kinetics. We conclude the paper with a summary of results.

2. The model

If the substrate is loaded uniaxially, stress is transferred from the substrate to the surface layer, and a tensile stress arises in the coating. This tensile stress may cause cracking of the coating. Generally, cracks grow perpendicular to the stress direction so that under uniaxial loading the cracks separate the coating into nearly rectangular independent fragments. The maximum of the stress and the strain in each fragment increases with the applied strain. Consequently, the continuous stretching of the substrate leads to multiple cracking and fragmentation of the coating. Since randomly distributed defects, e.g., microcracks, flaws and pores which occur during the manufacturing process, promote the breaking of the coating, the fragment lengths, i.e., the distances between neighbouring cracks, are statistically distributed as well. In this study, the evolution of the fragment length distribution with the applied strain is investigated. We assume that the substrate is elongated uniformly. Thus the substrate's strain is equal to the applied macroscopic strain. In an experimental situation, more material-specific features may complicate the situation, for example partial debonding of the fragments from the substrate, substrate yielding and non-uniform substrate deformation. In this article, these aspects are neglected as well as intrinsic stresses which may occur during the preparation of the coating.

The fact that the fragments are independent and the assumption of uniform substrate deformation allows calculation of the stress and strain in each fragment independently. Fig. 1 schematically depicts a fragment of length L and of thickness h_c that adheres to a substrate. The loading direction is parallel to the x axis. We assume that the tensile stress σ of the coating does not vary with the thickness of the coating and that the coating material is linear elastic with Hooke's constant E_c. Thus $\sigma = E_c\epsilon_c$ holds where $\epsilon_c(x)$ denotes the local strain in the coating. The substrate is uniformly elongated so that the substrate's strain $\epsilon_s(x)$ does not vary with x and equals the applied strain ε: $\epsilon_s(x) \equiv \varepsilon$. In a quasistatic situation, the forces acting on each coating element are in equilibrium and hence in a shear-lag picture [20] $[\sigma(x+dx) - \sigma(x)]h_c = \tau(x)\,dx$ holds for each coating element of length dx, where $\tau(x)$ denotes

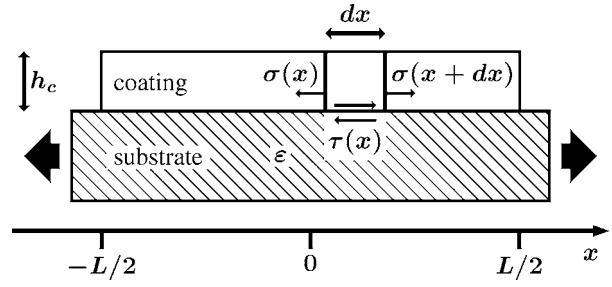

Figure 1 A fragment of length L that adheres to a substrate. The thickness of the coating is denoted by h_c. The substrate's strain is ε. The variable σ denotes the tensile stress in the coating, and $\tau(x)$ is the shear stress at the interface. The loading direction is parallel to the x axis.

the interfacial shear stress at position x. This yields

$$\frac{d\sigma}{dx} = \frac{\tau}{h_c} \tag{1}$$

In order to calculate the stress and the strain in the coating it is necessary to specify the stress–strain relation for the shear stress τ at the interface. In this study the influence of a nonlinear elastic stress–strain relation for the interfacial shear stress is analyzed in detail. This stress–strain relation is given by [21]

$$\tau(w) = \begin{cases} \operatorname{sgn}(w)C & \text{for} \quad m = 0 \\ Gw & \text{for} \quad m = 1 \\ BG[w/B + \operatorname{sgn}(w)|w/B|^m] & \text{for} \quad m > 1 \end{cases} \tag{2}$$

$$w(\tau) = \tau/G + \operatorname{sgn}(\tau)B|\tau/(BG)|^{1/m} \qquad \text{for} \quad 0 < m < 1,$$

where B, C and G are positive parameters and w is equal to the difference of the displacement $u_c(x)$ in the coating and the displacement $u_s(x) = \varepsilon x$ in the substrate: $w(x) = u_c(x) - \varepsilon x$. The parameter m plays the role of a nonlinearity parameter and strongly influences the shape of the stress–strain relation. Because of the nonlinear character of Equation 2, in this study the linear shear-lag model introduced by Cox [20] is generalized for nonlinear stress transfer. The stress–strain relation Equation 2 describes the stress transfer at the interface. The formal structure of Equation 2 is related to the Taylor expansion of functions. For small w, i.e., $|w| \ll B$ and $m > 0$, the stress–strain relation can be approximated by a linear relation between stress and strain (Hooke's law). For very large w ($|w| \gg B$) and $m > 0$, the power function term in Equation 2 dominates. For $m = 0$ the interfacial stress is constant, an assumption being made in previous studies on fragmentation of coatings and fibres [22–24]. Fig. 2 shows the dependence of τ on w for different m values: For $m = 0$ the interfacial stress is constant. The case $m = 1$ corresponds to Hooke's law (linear elastic stress transfer). For $m > 1$ the stress–strain relation has an increasing secant modulus, whereas for $0 < m < 1$ Equation 2 approximates the elastic part of the stress–strain curve for materials which have a yield point. Consequently, the stress–strain relation Equation 2 approximates the elastic response of a large class of

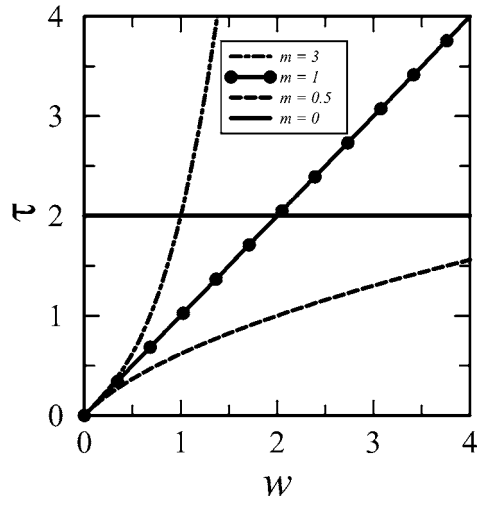

Figure 2 The interfacial shear stress–strain relation $\tau(w)$ for several m values. The parameters are $B=1$, $C=2$ and $G=1$, cf. Equation 2.

materials. Note that a similar expression for the (tensile) stress–strain relation of materials has been used by Ramberg and Osgood [25].

The displacement $u_c(x)$ in the coating and the coating's strain ϵ_c are related by $\epsilon_c = du_c/dx$. Inserting $\sigma = E_c\epsilon_c = E_c\, du_c/dx$ into Equation 1 yields

$$\frac{d^2u_c}{dx^2} = \frac{\tau(u_c - \varepsilon x)}{E_c h_c} \tag{3}$$

The edges of each fragment are free so that at the boundaries of each fragment the stress and the strain vanish: $du_c(x)/dx = 0$ for $|x| = L/2$ with $x = 0$ being the fragment's center. In the initial stage of fragmentation, the displacements $u_c(x)$ and $u_s(x)$ do not differ much. Therefore for $m > 0$ the stress–strain relation Equation 2 can be approximated by Hooke's law $\tau = Gw$. Then the solution of Equation 3 is given by $u_c(x) = \varepsilon x - \varepsilon\xi_1 \sinh(x/\xi_1)/\cosh[L/(2\xi_1)]$ with $\xi_1 = \sqrt{E_c h_c/G}$. The strain ϵ_c in the coating follows from $\epsilon_c = du_c/dx$:

$$\epsilon_c(x) = \varepsilon\left(1 - \frac{\cosh[x/\xi_1]}{\cosh[L/(2\xi_1)]}\right) \tag{4}$$

Note that for $\xi_1 \gg L$ Equation 4 simplifies to a parabola: $\epsilon_c(x) = \varepsilon L^2(1 - 4x^2/L^2)/(8\xi_1^2)$. For $m = 0$ Equation 3 yields $d\epsilon_c/dx = \mathrm{sgn}(w)C/(E_c h_c)$ and hence

$$\epsilon_c(x) = \begin{cases} \varepsilon & \text{for} \quad |x| \le L/2 - \xi_0 \\ LC(1 - |2x/L|)/(2E_c h_c) & \text{for} \quad |x| > L/2 - \xi_0 \end{cases} \tag{5}$$

with $\xi_0 = \varepsilon E_c h_c/C$. Equation 5 also holds for $\xi_0 > L/2$. The stress $\sigma(x)$ in the coating follows from $\sigma(x) = E_c\epsilon_c(x)$ for all m values. Fig. 3 depicts the function $\epsilon_c(x)$ for $m = 0$ and $m = 1$ and for two values of the ratio ξ_0/L and ξ_1/L respectively. In Fig. 3 the applied strain ε is set to 1%. The shape of the strain function ϵ_c depends on the nonlinearity parameter m and a characteristic length $\xi(m) \equiv \xi_m$ which is often denoted by

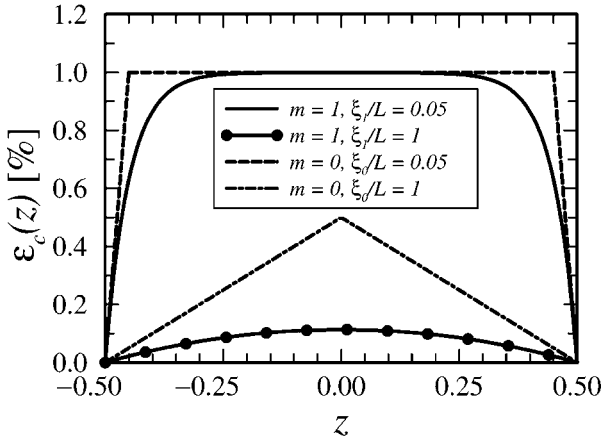

Figure 3 The strain ϵ_c in a fragment of length L as a function of $z = x/L$ for $m = 0$ and $m = 1$ and two $\xi(m)/L$ values, see also Equations 4 and 5. The value of ε is 1%.

exclusion zone, shield zone, stress transfer length, correlation length or screening length [22, 26–32]. If $\xi(m)$ is much smaller than the length of the fragment (which is typical for the initial stage of fragmentation), then the strain function depicts a plateau with $\epsilon_c = \varepsilon$. At the boundaries, the strain ϵ_c in the coating decreases to zero, for $m = 0$ linearly and for $m = 1$ exponentially. When the correlation length $\xi(m)$ is larger than the length of the fragment, the displacements $u_c(x)$ of the fragments are much smaller than the displacements $u_s(x)$ of the substrate so that $u_c - \varepsilon x \approx -\varepsilon x$ holds. In addition for $|w| \gg B$ the power function term in the interfacial shear stress–strain relation Equation 2 dominates. Thus inserting $w \approx -\varepsilon x$ and $\tau(w) \propto w^m$ into Equation 3 leads to $d\epsilon_c/dx = -G(\varepsilon x)^m/(E_c h_c B^{m-1})$ for $x > 0$ and

$$\epsilon_c(x) = \varepsilon^m L^{m+1} g_m(z) \tag{6}$$

with $g_m(z) = G(1 - |2z|^{m+1})/[2^{m+1}(m+1)E_c h_c B^{m-1}]$ and $z = x/L$ [33, 34]. Equation 6 is valid for all m values ($0 \le m < \infty$) and comprises the special cases $m = 0$ (after substituting G/B^{m-1} by C) and $m = 1$ for $\xi(m) \gg L$, see Equations 5 and 4. The "form factor" $h_m(z) = 1 - |2z|^{m+1}$ is displayed in Fig. 4. Note that the stress $\sigma(x)$ and the strain $\epsilon_c(x)$ are proportional to $h_m(z)$, and the maximum of the stress and the strain in

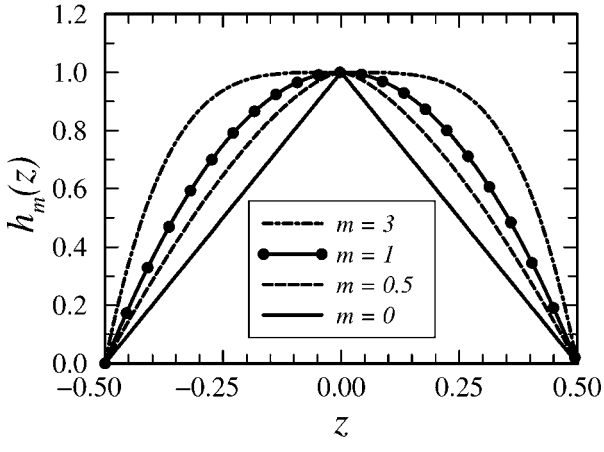

Figure 4 The "form factor" $h_m(z) = 1 - |2z|^{m+1}$ with $z = x/L$ for different m values. The strain $\epsilon_c(x)$ in a fragment of length L is proportional to $\varepsilon^m L^{m+1} h_m(z)$.

each fragment are proportional to L^{m+1}. The plateau with $\epsilon_c \equiv \varepsilon$ in the middle of the fragment disappears for $\xi(m) \gg L$ and $|w| \gg B$, and the strain $\epsilon_c(x)$ displays a noticeable maximum in the center of the fragment. For $m = 0$ the strain $\epsilon_c(x)$ increases linearly from the boundaries, and for $m = 1$ the shape of the strain function is parabolic. For very large m values, the function $\epsilon_c(x)$ depicts a plateau being proportional to $\varepsilon^m L^{m+1}$.

3. Analysis of the fragmentation process

Since small defects such as microcracks and pores cause a stress concentration if the sample is loaded, the random distribution of defects in the coating gives rise to a statistical distribution of the local strength of the coating. Within this picture, failure can be modelled by assuming that each element of the coating can only withstand a fixed value of stress or strain which is statistically distributed and which is prescribed in the beginning (quenched disorder). In this study, we assume that a crack occurs at position x when the strain $\epsilon_c(x)$ in the coating exceeds a local failure threshold $\epsilon_b(x)$. Because of the statistical distribution of the local strength, a fragment does not necessarily fail at the position of the strain maximum, but at the position where the local strain $\epsilon_c(x)$ exceeds $\epsilon_b(x)$. Since the distribution of defects is *a priori* unknown, it is necessary to make an assumption for the strength distribution. The weakest link approach assumes that the strength of materials is determined by the strength of its weakest element (link). Therefore the statistical aspects of failure phenomena are strongly associated with the statistics of extremes. In this context it has been shown that in the limit of a large number of links the statistics of minima converges to the Weibull distribution, if the strength distribution has a bounded tail [35] and if the failure distributions of all links are equal [36]. Following this idea we assume that the cumulative probability distribution for the local failure threshold $\epsilon_b(x)$ of a coating element of length Δx is given by a three parameter Weibull distribution:

$$P_\varepsilon(\epsilon_b) = 1 - \exp\left[-\Delta x \left(\frac{\epsilon_b - \epsilon_{\min}}{\omega}\right)^\alpha\right] \qquad (7)$$

for $\epsilon_b > \epsilon_{\min}$ and $P_\varepsilon(\epsilon_b) = 0$ otherwise. Here $\epsilon_{\min}$ and the scale parameter ω are positive and for the shape parameter $\alpha \geq 1$ holds. The corresponding strength distribution P_σ for a linear elastic coating with $\sigma = E_c\epsilon_c$ is $P_\sigma(\sigma_b) = 1 - \exp\{-\Delta x[(\sigma_b - \sigma_{\min})/(E_c\omega)]^\alpha\}$ where we set $\sigma_{\min} = E_c\epsilon_{\min}$. The behaviour of $P_\varepsilon(\epsilon_b)$ for small values of ϵ_b is essential for failure in large systems: In this limit, $P_\varepsilon(\epsilon_b) \propto (\epsilon_b - \epsilon_{\min})^\alpha$ holds. Thus the Weibull function is intimately related to power functions [37].

3.1. Initial stage of fragmentation

In section 2 the strain distribution in an arbitrary fragment was obtained. In the following the initial and the later stage of fragmentation are discussed. Neglecting the exclusion zone close to the fragments' boundaries, the coating's strain equals the applied strain in the initial stage of breaking: $\epsilon_c \equiv \varepsilon$. Using this approximation, one can derive the probability that a fragment of length L fails under the applied macroscopic strain ε. We set $s = [(\varepsilon - \epsilon_{\min})/\omega]^\alpha$. If a coating element of length Δx has withstood the applied load s with $\varepsilon > \epsilon_{\min}$, then it fails under the applied load s^* with the probability

$$P(\Delta x, s^*|s) = 1 - \exp[-(s^* - s)\Delta x] \qquad (8)$$

The probability $P_-(L, s^*|s)$ that a crack occurs in a fragment of length L at the load s^* under the assumption that the whole fragment has withstood the applied load s follows from the probability that each of the coating elements fails: $P_-(L, s^*|s) = 1 - \prod_i [1 - P(\Delta x_i, s^*|s)] = 1 - \exp[-L(s^* - s)]$ with $\sum_i \Delta x_i = L$. Therefore the density $p_-(L, s)$ of the probability that a fragment of length L fails under the incremental increase ds of the load is

$$p_-(L, s) = \left.\frac{\partial P_-(L, s^*|s)}{\partial s^*}\right|_{s^*=s} = L \qquad (9)$$

if the fragment has survived the applied load s. If a fragment has withstood the external load s, then a crack occurs in the interval x to $x + \Delta x$ with the probability $P_+(x, s^*|s)$. This probability is equal to the probability that the coating element at position x fails times the probability that the other elements of the fragment stay intact: $P_+(x, s^*|s) = (1 - \exp[-(s^* - s)\Delta x]) \exp[-\int_0^x (s^* - s)\,dx - \int_{x+\Delta x}^L (s^* - s)\,dx]$. Expanding the exponential term yields $P_+(x, s^*|s) = \Delta x(s^* - s) \exp[-L(s^* - s)]$ for very small Δx. The corresponding density $p_+(x, L, s)$ of the probability that a fragment of length L fails between x and $x + \Delta x$ after an incremental load increase ds and after having withstood s is:

$$p_+(x, L, s)\,\Delta x = \left.\frac{\partial P_+(x, s^*|s)}{\partial s^*}\right|_{s^*=s} = \Delta x \qquad (10)$$

Because of the continuous elongation of the substrate multiple cracks occur in the coating, and rectangular fragments are formed. The pattern of cracks is characterized by the distribution of the fragment lengths, i.e., the distances between neighbouring failures. During fragmentation, existing fragments break up and new fragments are created so that the fragment length distribution is a function of the applied strain. The evolution of the number density $n(L, s)$ of fragments with length L is determined by the breakup of existing fragments of length L and the formation of new fragments of length L by the breakup of fragments which are larger than L. Since $p_-(L, s)$ denotes the density of the probability that a fragment of length L breaks and $p_+(L, x, s)$ is the density of the probability that a fragment of length x breaks at position L within the fragment, we find [38, 39]

$$\frac{\partial n(L, s)}{\partial s} = -p_-(L, s)n(L, s) + 2\int_L^\infty p_+(L, x, s)n(x, s)\,dx \qquad (11)$$

Here we assume that every breakage event is associated with one crack in each fragment only. The fragment length distribution $\rho(L,s)$ is obtained by normalising the number density $\rho(L,s)=n(L,s)/\int_0^\infty n(L,s)\,dL$, and the average fragment length follows from $\langle L\rangle=\int_0^\infty L\,\rho(L,s)\,dL$.

The initial length of the intact coating is denoted by L_0. Inserting the probability densities $p_-(L,s)$ and $p_+(x,L,s)$ into the kinetic Equation 11 leads to an evolution equation for the number density $n(L,s)$ of fragments:

$$\frac{\partial n(L,s)}{\partial s}=-n(L,s)L+2\int_L^{L_0} n(x,s)\,dx \qquad (12)$$

Note that in Equation 12 the integration range only extends to L_0, since the initial length of the coating is L_0 and consequently there are no fragments that are larger than L_0. For $\varepsilon\le\epsilon_{\min}$ only the intact coating exists. Therefore the initial condition is given by $n(L,0)=\delta(L-L_0)$. Then the solution of Equation 12 for $\varepsilon>\epsilon_{\min}$ is $n(L,s)=[\delta(L-L_0)+2s+s^2(L_0-L)]\exp(-Ls)$ for $0\le L\le L_0$ and $n(L,s)\equiv 0$ for $L>L_0$ [38]. Here $\delta(x)$ denotes Dirac's delta function. Normalising the function $n(L,s)$, one finds for the fragment size distribution $\rho(L,s)$ in the range $0\le L\le L_0$ and for $\varepsilon>\epsilon_{\min}$

$$\rho(L,s)=\frac{\left[\delta(L-L_0)+2s+s^2(L_0-L)\right]\exp(-Ls)}{1+L_0 s} \qquad (13)$$

The mean fragment length is given by $\langle L\rangle=L_0/(1+L_0 s)$. The average number of cracks in the initial stage ($\epsilon_c\equiv\varepsilon$) is $[L_0P_\varepsilon(\varepsilon)]/\Delta x\approx L_0 s$ if one linearizes the Weibull function in Equation 7 near $\epsilon_{\min}$. For $L\ll L_0$ and a large number of cracks ($L_0 s\gg 1$) one has $\rho(L,s)=s\exp(-Ls)$. Therefore in the initial stage of fragmentation, the fragment lengths are approximately exponentially distributed. The average fragment length is given by $\langle L\rangle=1/s=[\omega/(\varepsilon-\epsilon_{\min})]^\alpha$. Consequently, the mean fragment length $\langle L\rangle$ scales with the applied strain in the initial stage of fragmentation:

$$\langle L\rangle\propto(\varepsilon-\epsilon_{\min})^{-\kappa_1} \qquad (14)$$

with $\kappa_1=\alpha$. Note that for a linear elastic substrate $\langle L\rangle\propto(\sigma_s-E_s\epsilon_{\min})^{-\alpha}$ holds where $\sigma_s=E_s\varepsilon$ is the substrate's stress and E_s denotes the elasticity constant of the substrate. These results for the special case $\epsilon_{\min}=0$ have been already derived in [24, 40–44]. Interestingly, the scaling exponent κ_1 only depends on the disorder parameter α of the failure threshold distribution Equation 7. Thus the evolution of $\langle L\rangle$ with the applied strain ε in the initial cracking regime allows determination of the lower bound $\epsilon_{\min}$ of the failure threshold distribution and the Weibull parameters α and ω.

3.2. Later stage of fragmentation

For $\xi(m)\gg L$ and $|w|\gg B$ (which is typical for the later stages of the breaking process) the strain in the coating attains a more complex form, see Equation 6. A previous study [34] has shown that the approach for deriving the failure probability densities Equations 9 and 10 can be generalized for the special case $\epsilon_{\min}=0$ if the strain attains the scaling form Equation 6 and under the assumption that the fragment is loaded monotonically from 0 to s^*. After each breakage event in the later cracking regime the stress and the strain in the fragment that failed relaxes since the maxima of the stress and the strain are proportional to L^{m+1}, see Equation 6. Therefore the stress and the strain in a fragment strongly decay if a crack occurs in the fragment and creates two new fragments with smaller fragment lengths than the length of the original fragment. Consequently, the derivation of failure probabilities in the later cracking stages must take into account the non-monotonic stress and strain history of the fragments. If one neglects this non-Markovian character of fragmentation, then the derived probabilities only approximate the true failure probabilities, and the kinetic Equation 11 itself only approximates the evolution of the fragment size distribution [34]. In this work a numerical approach which takes into consideration the stress and strain history of the fragments is applied to obtain the fragmentation length distribution. Since in [27] the authors have shown that the fragment length distribution for $\epsilon_{\min}>0$ in the later cracking stages is non-universal and depends on the distribution of cracks which were created in the initial stage of fragmentation, in the following the distribution of the fragment sizes is considered only for the case $\epsilon_{\min}=0$.

In order to simulate the sequential breaking of the coating, the coating is divided into N links. In the beginning, for each element of the coating a value of the failure threshold ϵ_b is fixed based on the probability distribution Equation 7. The strain in each fragment and in the coating before the first failure can be calculated using Equation 6. Because of the scaling form of Equation 6 with respect to ε one can compute easily the first and the following links which break for the chosen realization of the probability distribution Equation 7. Noting the broken links, one can determine the fragment size distribution.

The results of the simulations of the fragmentation process are presented in Figs 5 and 6. Fig. 5 displays the fragment length distribution for $\epsilon_{\min}=0$ and (a) $m=0.05$, (b) $m=1$ and (c) $m=9$ in the later stage of the fragmentation process. The Weibull shape parameter α is set to $\alpha=5$ and $\alpha=9$ respectively, and the number N of links is $N=2\times10^6$. Moreover in the simulations $E_c h_c B^{m-1}/G=10^{12}$ was used. The fragment size distribution after 10000 failures is plotted as a function of $\zeta=L/\langle L\rangle$ and was obtained by averaging over the results of 5 simulations based on the Weibull distribution Equation 7. Previous works have shown [21, 26–28, 34] that for $\epsilon_{\min}=0$ the rescaled fragment length distribution $p(\zeta)$ of the later cracking regime is a function of m and α only and does not depend on the applied strain ε anymore. The simulations reveal that the fragment size distribution depicts a maximum and is roughly centered around $\zeta=1$ corresponding to $L=\langle L\rangle$. The maximum of $p(\zeta)$ is more pronounced with decreasing m. This behaviour can be explained by

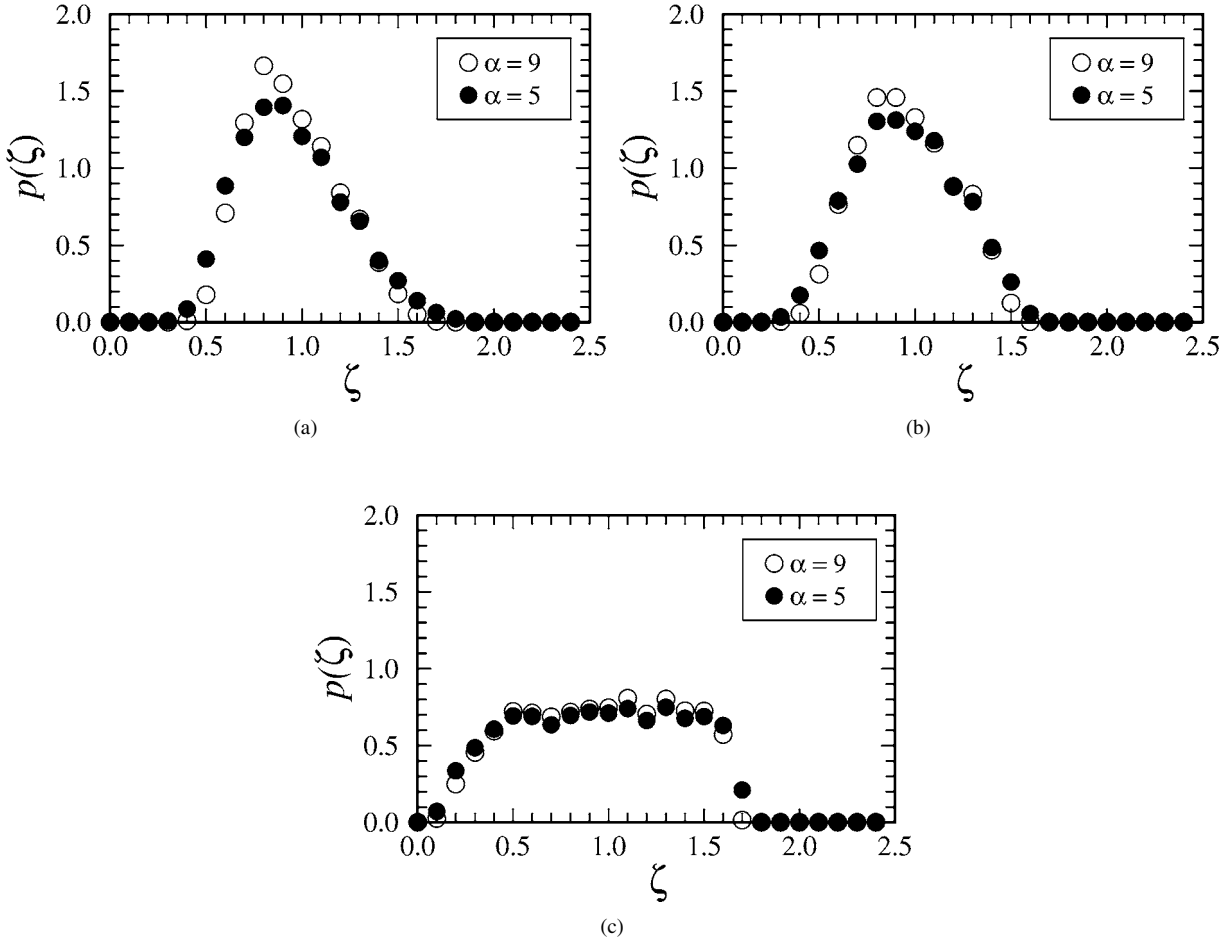

Figure 5 The rescaled fragment length distribution $p(\zeta)$ with $\zeta = L/\langle L\rangle$ in the later stage of the fragmentation process after 10000 breakage events for $\epsilon_{\min} = 0$, $\omega = 5 \times 10^{-3}$, $E_c h_c B^{m-1}/G = 10^{12}$ as well as $\alpha = 5$ and $\alpha = 9$ respectively. The value of the nonlinearity parameter is (a) $m = 0.05$, (b) $m = 1$ and (c) $m = 9$. For each set of parameters 5 simulations based on the Weibull distribution Equation 7 were run. The function $p(\zeta)$ was obtained by averaging over the results of these 5 runs.

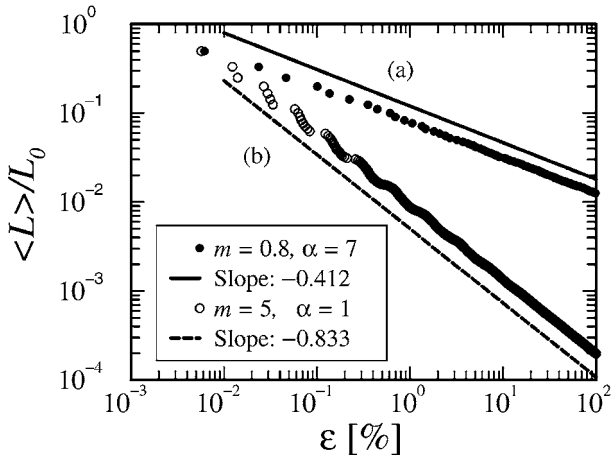

Figure 6 The average fragment length $\langle L\rangle$ vs. applied strain ε in the later cracking stages for the parameters (a) $m = 0.8$, $\epsilon_{\min} = 0$, $\omega = 10^{-4}$, $\alpha = 7$, $E_c h_c B^{m-1}/G = 10^{12}$ and (b) $m = 5$, $\epsilon_{\min} = 1\%$, $\omega = 10^{-3}$, $\alpha = 1$, $E_c h_c B^{m-1}/G = 10^{16}$ in systems with $N = 2 \times 10^6$ links. Each curve is obtained by averaging the results of 10 simulations based on the probability distribution Equation 7. The slope of the solid line is -0.412, the slope of the dashed line is -0.833, see text for details.

the shape of the strain distribution Equation 6. For low m values, $\epsilon_c(x)$ has a noticeable maximum. For larger m values the function $\epsilon_c(x)$ displays a plateau so that the failure probability ceases to depend on x. Comparing the fragment length distributions for a fixed m value and different values of α in Figs 5a–c, the influence of the shape parameter α on the fragment length distribution becomes obvious: Increasing the α value results in a larger maximum of the fragment length distribution, since increasing α also implies less scattering of ϵ_b.

Fig. 6 displays the average fragment length $\langle L\rangle$ as a function of the applied strain ε for the parameters (a) $m = 0.8$, $\epsilon_{\min} = 0$, $\omega = 10^{-4}$, $\alpha = 7$, $E_c h_c B^{m-1}/G = 10^{12}$ and (b) $m = 5$, $\epsilon_{\min} = 1\%$, $\omega = 10^{-3}$, $\alpha = 1$, $E_c h_c B^{m-1}/G = 10^{16}$. The number of links is $N = 2 \times 10^6$. Each curve is obtained by averaging the results of 10 simulations based on the probability distribution Equation 7. Both curves clearly reveal that $\langle L\rangle$ scales with ε [33, 45]:

$$\langle L\rangle \propto \varepsilon^{-\kappa_2} \tag{15}$$

This scaling behaviour in the later stage of the cracking process can be explained by considering the characteristic length scale [33]: For each value of the applied strain ε there exists a characteristic length $L_c(\varepsilon)$ so that fragments of length $L_c(\varepsilon)$ stay intact with the probability of 50%. This probability is given by

$$\exp\left\{-2\int_{x_{\min}}^{L_c/2}\left[\frac{\epsilon_c(x)-\epsilon_{\min}}{\omega}\right]^{\alpha} dx\right\} = 0.5 \tag{16}$$

where $x_{\min}$ is defined by $\varepsilon^m [L_c(\varepsilon)]^{m+1} g_m(x_{\min}/L) = \epsilon_{\min}$ with $x_{\min} > 0$. Inserting $\epsilon_c(x) = \varepsilon^m [L_c(\varepsilon)]^{m+1}$

$g_m(z)$ (Equation 6) into Equation 16 yields $L_c(\varepsilon) = \text{const} \cdot \varepsilon^{-m\alpha/[(m+1)\alpha+1]}$ for $\epsilon_{\min} = 0$. In this case the value $L_c(\varepsilon)(\epsilon_{\min}/\omega)^{\alpha}$ is zero which corresponds to a strongly disordered situation [26–28, 33]. Assuming that the mean fragment size $\langle L \rangle$ is proportional to $L_c(\varepsilon)$, we find the scaling relation $\langle L \rangle \propto \varepsilon^{-\kappa_2}$ with [33]

$$\kappa_2 = m\alpha/[(m+1)\alpha + 1] \tag{17}$$

The case where the value of $L_c(\varepsilon)(\epsilon_{\min}/\omega)^{\alpha} \gg 1$ is large belongs to the so-called weak disorder situation [26–28, 33]. Then the cracks occur close to the centers of the fragments when $\epsilon_c(0) \approx \epsilon_{\min}$ holds. This implies for the characteristic length $\epsilon_c(0) = \varepsilon^m [L_c(\varepsilon)]^{m+1} g_m(0) \approx \epsilon_{\min}$ and thus $\langle L \rangle \propto L_c(\varepsilon) \propto \varepsilon^{-\kappa_2}$ where

$$\kappa_2 = m/(m+1) \tag{18}$$

holds [33]. Consequently, in weakly and in strongly disordered systems the average fragment length $\langle L \rangle$ also scales with ε in the later cracking stages. In this regime, the power law exponent depends on the nonlinearity parameter m of the stress–strain relation Equation 2. Since the scaling law exponent κ_1 of the initial cracking regime only depends on the shape parameter of the Weibull distribution Equation 7 and the power law exponent κ_2 on m, one can experimentally determine the parameters of the Weibull function and the nonlinearity parameter m from the evolution of the average fragment length with the applied strain.

The simulations of the later cracking stages confirm the scaling law Equation 15. A least-squares fit to the curves in the ε range 1% to 100% in Fig. 6 lead to (a) $\kappa_2 = 0.400 \pm 0.001$ being close to the theoretical value of Equation 17 $\kappa_2 = 0.412$. In Fig. 6b the numerical result is $\kappa_2 = 0.836 \pm 0.000$ which has to be compared with $\kappa_2 = 0.833$, see Equation 18. In conclusion, the simulation results agree very well with the analytical results Equations 17 and 18.

4. Conclusions

In this study, the influence of a nonlinear elastic stress transfer mechanism on the fragmentation of coatings under uniaxial loading was investigated. Analyzing a shear-lag model, the stress and the strain in the coating as a function of the substrate's strain were derived. In the initial stage of fragmentation, the coating's strain equals the substrate's strain everywhere beside the exclusion zone at the fragments' edges. In the later cracking stages, the stress and the strain attain a universal scaling form. The statistical distribution of the local strength of the coating was taken into account by a three parameter Weibull distribution for the local failure threshold of the coating's strain. In the initial stage of cracking, the fragments are approximately exponentially distributed. The mean fragment length in the initial stage of cracking decays with a power law where the power law exponent is equal to the Weibull shape parameter. In this initial regime, the evolution of the mean fragment length with the applied strain allows determination of the parameters of the Weibull distribution. The results of the simulations for the later fragmentation stages reveal that the fragment length distribution displays a noticeable maximum for the parameter values chosen. The width of the rescaled fragment length distribution increases with increasing values of the nonlinearity parameter of the interfacial shear stress–strain relation. The average fragment length also scales with the applied strain in the later stages of cracking. In this regime, the scaling exponent depends on the nonlinearity parameter of the interfacial shear stress–strain relation and the parameters of the strength distribution. By combining the results of measurements of the initial and the later cracking stages, one can determine experimentally the parameters of the Weibull distribution and the nonlinearity parameter. In conclusion, the analysis of the fragmentation kinetics allows both the degree of disorder in the coating and the mechanical properties of the interface to be probed.

Acknowledgements

The discussions with Prof. Dr. A. Blumen and Prof. Dr. I. M. Sokolov are gratefully acknowledged.

References

1. J. W. HUTCHINSON and Z. SUO, *Adv. Appl. Mech.* **29** (1992) 63.
2. M. S. HU and A. G. EVANS, *Acta Metall.* **37** (1989) 917.
3. D. C. AGRAWAL and R. RAJ, *ibid.* **37** (1989) 1265.
4. J. A. NAIRN and S.-R. KIM, *Eng. Fract. Mech.* **42** (1992) 195.
5. D. R. WHEELER and H. OSAKI, in "Metallization of Polymers," edited by E. Sacher, J.-J. Pireaux and S. P. Kowalczyk (ACS Symposium Series **440**, Washington D.C., 1990), p. 500.
6. M. YANAKA, Y. TSUKAHARA, N. NAKASO and N. TAKEDA, *J. Mater. Sci.* **33** (1998) 2111.
7. X. F. YANG and K. M. KNOWLES, *J. Amer. Ceram. Soc.* **75** (1992) 141.
8. R. B. HENSTENBURG and S. L. PHOENIX, *Polym. Composites* **10** (1989) 389.
9. M. D. THOULESS, E. OLSSON and A. GUPTA, *Acta Metall. Mater.* **40** (1992) 1287.
10. Y. LETERRIER, D. PELLATON, D. MENDELS, R. GLAUSER, J. ANDERSONS and J.-A. E. MÅNSON, *J. Mater. Sci.* **36** (2001) 2213.
11. J. WALKER, *Sci. Am.* **255**(4) (1986) 178.
12. G. KORVIN, *Pure Appl. Geophys.* **131** (1989) 289.
13. U. A. HANDGE, Y. LETERRIER, J.-A. E. MÅNSON, I. M. SOKOLOV and A. BLUMEN, *Europhys. Lett.* **48** (1999) 280.
14. W. A. CURTIN and H. SCHER, *Phys. Rev. B* **45** (1992) 2620.
15. J. I. KATZ, *J. Appl. Phys.* **84** (1998) 1928.
16. B. EPSTEIN, *ibid.* **19** (1948) 140.
17. D. E. GÜCER and J. GURLAND, *J. Mech. Phys. Solids* **10** (1962) 365.
18. R. H. DOREMUS, *J. Appl. Phys.* **54**(9) (1983) 193.
19. C.-Y. HUI, S. L. PHOENIX and D. SHIA, *Compos. Sci. Technol.* **57** (1997) 1707.
20. H. L. COX, *Br. J. Appl. Phys.* **3** (1952) 72.
21. U. A. HANDGE, in "Statistische Aspekte der Fragmentierung von Oberflächenschichten" (in German) (Ph.D. Dissertation, University of Freiburg, Freiburg i. Brsg. (Germany), 2000) p. 13.
22. W. A. CURTIN, *J. Mater. Sci.* **26** (1991) 5239.
23. Y. LETERRIER, Y. WYSER, J.-A. E. MÅNSON and J. HILBORN, *J. Adhesion* **44** (1994) 213.
24. C.-Y. HUI, S. L. PHOENIX, M. IBNABDELJALIL and R. L. SMITH, *J. Mech. Phys. Solids* **43** (1995) 1551.
25. W. RAMBERG and W. R. OSGOOD, in "National Advisory Committee for Aeronautics: Technical Note No. 902" (1943).
26. O. MORGENSTERN, I. M. SOKOLOV and A. BLUMEN, *Europhys. Lett.* **22** (1993) 487.
27. *Idem.*, *J. Phys.* A **26** (1993) 4521.
28. I. M. SOKOLOV, O. MORGENSTERN and A. BLUMEN, *Macromol. Symp.* **81** (1994) 235.

29. J. C. GROSSKREUTZ and M. B. MCNEIL, *J. Appl. Phys.* **40** (1969) 355.
30. H. COLINA, L. DE ARCANGELIS and S. ROUX, *Phys. Rev. B* **48** (1993) 3666.
31. T. HORNIG, I. M. SOKOLOV and A. BLUMEN, *Phys. Rev. E* **54** (1996) 4293.
32. C. Y. HUI, D. SHIA and L. A. BERGLUND, *Compos. Sci. Technol.* **59** (1999) 2037.
33. U. A. HANDGE, I. M. SOKOLOV and A. BLUMEN, *Phys. Rev. E* **61** (2000) 3216.
34. J. ANDERSONS, U. A. HANDGE, I. M. SOKOLOV and A. BLUMEN, *Eur. Phys. J. B* **17** (2000) 261.
35. E. J. GUMBEL, in "Statistical theory of extreme values and some practical applications," Applied Mathematics Series **33** (U.S. Department of Commerce, National Bureau of Standards, Washington D.C., 1954).
36. M. R. GURVICH, A. T. DIBENEDETTO and S. V. RANADE, *J. Mater. Sci.* **32** (1997) 2559.
37. W. WEIBULL, *J. Appl. Mech.* **18** (1951) 293.
38. R. ENGLMAN, *J. Phys.: Condens. Matter* **3** (1991) 1019.
39. P. A. MULHERAN, *Philos. Mag. Lett.* **68** (1993) 63.
40. H. D. WAGNER and A. EITAN, *Appl. Phys. Lett.* **56** (1990) 1965.
41. J. ANDERSONS and V. TAMUŽS, *Compos. Sci. Tech.* **48** (1993) 57.
42. M. R. GURVICH, A. T. DIBENEDETTO and A. PEGORETTI, *J. Mater. Sci.* **32** (1997) 3711.
43. W. K. BROWN, R. R. KARPP and D. E. GRADY, *Astrophys. Space Sci.* **94** (1983) 401.
44. A. MÉZIN, J. LEPAGE, N. PACIA and D. PAULMIER, *Thin Solid Films* **172** (1989) 197.
45. U. A. HANDGE, Y. LETERRIER, G. ROCHAT, I. M. SOKOLOV and A. BLUMEN, *Phys. Rev. E* **62** (2000) 7807.

Received 11 March
and accepted 20 June 2002